Langmuir
Article
pubs.acs.org/Langmuir

Designing Oscillating Cilia That Capture or Release Microscopic Particles

Rajat Ghosh,[†] Gavin A. Buxton,[‡] O. Berk Usta,[§] Anna C. Balazs,[§] and Alexander Alexeev*,[†]

[†]George W. Woodruff School of Mechanical Engineering, Georgia Institute of Technology, Atlanta, Georgia 30332, [‡]Department of Science, Robert Morris University, Pittsburgh, Pennsylvania 15108, and [§]Chemical Engineering Department, University of Pittsburgh, Pittsburgh, Pennsylvania 15261

Received August 6, 2009. Revised Manuscript Received September 1, 2009

We use computational modeling to capture the three-dimensional interactions between oscillating, synthetic cilia and a microscopic particle in a fluid-filled microchannel. The synthetic cilia are elastic filaments that are tethered to a substrate and are actuated by a sinusoidal force, which is applied to their free ends. The cilia are arranged in a square pattern, and a neutrally buoyant particle is initially located between these filaments. Our computational studies reveal that, depending on frequency of the beating cilia, the particle can be either driven downward toward the substrate or driven upward and expelled into the fluid above the cilial layer. This behavior mimics the performance of biological cilia used by certain marine animals to extract suspended food particles. The findings uncover a new route for controlling the deposition of microscopic particles in microfluidic devices.

Introduction

A variety of marine animals use elastic hair-like filaments, or cilia, to capture food particles that are suspended in the surrounding solution.[1−4] These motile, microscopic cilia experience the surrounding medium as a low Reynolds number fluid,[2] i.e., a highly viscous environment, where the effects of inertia are negligible. Nevertheless, by oscillating in a periodic, time-irreversible manner, the cilia can generate net currents within the fluid and thereby, effectively pump the food particles toward the feeding animals. The behavior of these biological cilia provides a useful design concept for creating microfluidic devices where actuated "synthetic cilia" would regulate the movement of microscopic particles (e.g., biological cells or polymeric microcapsules) within the device.

The development of microfluidic channels that encompass synthetic cilia is still in its infancy;[5−8]nonetheless, recent experiments[5] demonstrated that actuated polymeric cilia are effective at pumping fluids within a prototypical device. Furthermore, recent studies involving nanoscale synthetic cilia showed that these filaments can dynamically interact with nanoscopic particles.[9] These experiments represent a technological drive for making microfluidic devices more responsive and, in particular, for creating the next generation of reconfigurable substrates for these devices. By designing responsive surfaces that encompass digit-like features that extend away from the surface and act as minute, mobile fingers, the devices could enable "on demand" trapping and release of nano- to microscopic particles. More generally, such responsive filaments could give rise to a microfluidic system that can sense local variations in the solution conditions (e.g., flow conditions) and autonomously adapt to these changes by altering its behavior.

To facilitate the design of the next stage devices, there is a need for computational studies that not only pinpoint the parameter space where the synthetic cilia would be most efficient, but also bring to light new functions that these filaments could perform. To date, there have been few simulations of the motion of microscopic particles in the three-dimensional fluid flow that is generated by the beating of cilia, and the potential functionality of synthetic filaments in the selective trapping of particles from the solution or the expulsion of trapped species remains unexplored.

Herein, we use three-dimensional computer simulations to probe the utility of harnessing a ciliated surface to transport microscopic solid particles within a fluid-filled microchannel, where the fluid is characterized by a low Reynolds number (Re). In this synthetic system, the cilia are elastic filaments that are tethered to a wall and actuated by externally applied forces. We introduce a neutrally buoyant, solid particle of radius R, which is sufficiently small (compared to the cilium length and intercilium distances) that the particle can move freely inside the ciliated layer. The micrometer-scale particle and cilia are sufficiently large, however, that they are not affected by Brownian fluctuations. As we show below, the actuated motion of these synthetic cilia can cause the particle to move perpendicular to the cilial layer. Furthermore, by changing the frequency of the applied force, we can regulate the direction of the particle's migration. In effect, this synthetic system mimics the ability of the marine suspension-feeders to manipulate particulates in their environment and can be utilized to facilitate either the deposition or removal of particles from substrates in microfluidic devices.

Methodology

Our simulation box encompasses four oscillating cilia and a suspended particle, which are immersed in a viscous fluid (see Figure 1). To capture the complex fluid−structure interactions in this multicomponent system, we employ our hybrid

*Corresponding author.

(1) Riisgard, H. U.; Larsen, P. S. *Limnol. Oceanogr.* **2001**, *46*, 882–891and references therein.
(2) Sleigh, M. A. *Comp. Biochem. Physiol., Part A: Physiol.* **1989**, *94*, 359–364.
(3) Mayer, S. *Bull. Math. Biol.* **2000**, *62*, 1035–1059.
(4) Grunbaum, D.; Eyre, D.; Fogelson, A. *J. Exp. Biol.* **1998**, *201*, 2575–2589.
(5) den Toonder, J.; Bos, F.; Broer, D.; Filippini, L.; Gillies, M.; de Goede, J.; Mol, T.; Reijme, M.; Talen, W.; Wilderbeek, H.; Khatavkar, V.; Anderson, P. *Lab Chip* **2008**, *8*, 533–541.
(6) Oh, K.; Chung, J. H.; Devasia, S.; Riley, J. J. *Lab Chip* **2009**, *9*, 1561–1566.
(7) Baltussen, M.; Anderson, P.; Bos, F.; den Toonder, J. *Lab Chip* **2009**, *9*, 2326–2331.
(8) van Oosten, C. L.; Bastiaansen, C. W. M.; Broer, D. J. *Nat. Mater.* **2009**, *8*, 677–682.
(9) Pokroy, B.; Kang, S. H.; Mahadevan, L.; Aizenberg, J. *Science* **2009**, *323*, 237–240.

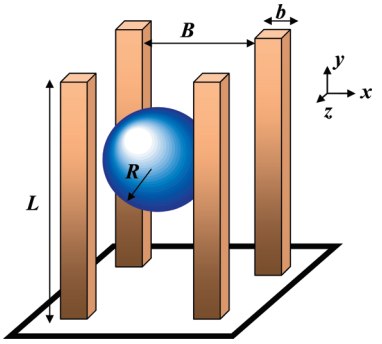

Figure 1. Schematic showing the three-dimensional arrangement of the cilia and the location of the spherical particle within the system.

"LBM/LSM" approach,[10−14] which integrates the lattice Boltzmann model (LBM)[15] for the hydrodynamics of viscous incompressible fluids and the lattice spring model (LSM)[16,17] for the micromechanics of elastic solids.

The LBM can be thought of as an efficient solver for the Navier−Stokes equation. More specifically, this lattice-based model consists of two processes: the propagation of fluid "particles" to neighboring lattice sites, and the subsequent collisions between particles when they reach a site. Here, the fluid particles are representative of mesoscopic portions of the fluid, and are described by a particle distribution function $f_i(\mathbf{r},t)$, which characterizes the mass density of fluid particles at a lattice node $\mathbf{r}$ and time t propagating in the direction i with a constant velocity $\mathbf{c}_i$. The time evolution of these distribution functions is governed by a discretized Boltzmann equation.[15]In three-dimensional systems, the simulations involve a set of 19 particle velocity distribution functions at each node. The hydrodynamic quantities are moments of the distribution function, i.e., the mass density $\rho = \Sigma_i f_i$, the momentum density $\mathbf{j} = \rho\mathbf{u} = \Sigma_i \mathbf{c}_i f_i$, with $\mathbf{u}$ being the local fluid velocity, and the momentum flux $\Pi = \Sigma_i \mathbf{c}_i \mathbf{c}_i f_i$.

Via the LSM, we can fashion the cilia and the particle from a network of harmonic "springs", which connect nearest and next-nearest neighbor lattice nodes (see below). We assign a mass M_i to each LS node at position $\mathbf{r}_i$ and integrate Newton's equation of motion, $\mathbf{F}(\mathbf{r}_i) = M_i(d^2\mathbf{r}_i/dt^2)$, where $\mathbf{F}$ is the total force acting on the node. Specifically, $\mathbf{F}$ consists of the force due to the interconnecting springs and the force exerted by the fluid on the solid at the solid−fluid boundary. The velocity Verlet algorithm is used to integrate this equation of motion.[18]

In our LBM/LSM simulations, the fluid and solid phases interact through appropriate boundary conditions.[10−14] In particular, lattice spring nodes that are situated at the solid−fluid interface impose their velocities on the surrounding fluids; the velocities are transmitted through a modified bounce-back rule[19] to those LBM distribution functions that intersect the moving solid boundary. In turn, LS nodes at the solid−fluid interface experience forces due to the fluid pressure and viscous stresses at that boundary. We calculate the latter force based on the momentum exchange between the LBM particle and solid boundary and then distribute this quantity as a load to the neighboring LS nodes.

We construct each cilium from cubic elementary LSM units to form an elastic beam, which has a length of $L = 4R$, and a width of $b = 0.1L$. The intercilium separation is $B = 3R$. Given that k is the spring constant of the interconnecting harmonic springs,[20] the Young's modulus of the cilium is $E = 5k/2\Delta x_{LS}$ and the solid density is $\rho_s = M/\Delta x_{LS}^3$, where $\Delta x_{LS} = L/30$ is the spacing between the LS nodes.[13,17] We set the Young's modulus $E = 1$ and density $\rho_s = 1$ (in LB units). This simple lattice model is restricted to a Poisson's ratio of 1/4, which is in the range of experimentally realistic values.[21,22] We note that more complicated many-body interactions can be included in our model to vary the Poisson's ratio.[17]

The particle's three-dimensional shell is constructed from two concentric layers of LS nodes.[14] By using the Delaunay triangulation technique,[23] we distribute nodes in a regular manner on each surface. These two concentric surfaces are separated by a distance that is equal to the average size of a triangular bond and are connected by springs between the nearest and next nearest neighbor nodes. The spring constant for springs located on the capsule surfaces and normal to the surfaces is k, while the diagonal springs have spring constants of $2/3k$. The particle has a radius of $R = 10$ (with $N_0 = 642$ nodes on the surface), a shell thickness of $\Delta x_c \approx 1.4$, and density of $\rho_s = 1$. The Young's modulus of the shell is $E \approx 5/18$.

To prevent overlap between the capsule and the cilium, we introduce the following Morse potential: $\phi(r) = \varepsilon(1 - \exp[-(r - r_0)/\kappa])^2$. Here, ε and κ characterize the respective strength and range of the interaction potential, and r is the distance between a pair of LS nodes, where one node lies on the capsule's outer surface and the other lies at the cilium−fluid interface. The parameter $r_0 = 1.8$ is the equilibrium distance where the force due to the potential is zero. We fix $\varepsilon = \varepsilon_r = 0.005$ for the repulsive part of the potential ($r < r_0$), while for the attractive part ($r > r_0$), we set $\varepsilon = 0$. In addition, $\kappa = 1$. Note all numbers are in LBM units.

Each cilium is driven by an oscillatory force that is applied to its free end. This sinusoidal force, which sets the entire system into periodic motion, is directed along the x-axis and has a frequency f and a dimensionless amplitude $A = (1/3)aL^2/EI$ that represents the ratio between the amplitude of the external driving force and the bending rigidity of a elastic cilium. Here, a is the force amplitude, and $I = b^4/12$ is the cilium's moment of inertia. In the ensuing simulations, we set $A = 1$. In other words, we assume that the driving force on the cilia is comparable to the elastic response of the filament. For this ratio, the motion of the cilia remains primarily planar; furthermore, the cilia do not undergo buckling or hit the substrate as they undergo their oscillations.[13]

In the field of hydrodynamics, it is common practice to characterize the properties of the system by dimensionless numbers, which represent ratios of the salient influences (e.g., the dimensionless Reynolds number of a fluid represents the relative

(10) Alexeev, A.; Verberg, R.; Balazs, A. C. *Macromolecules* **2005**, *38*, 10244–10260.
(11) Alexeev, A.; Verberg, R.; Balazs, A. C. *Phys. Rev. Lett.* **2006**, *96*, 148103.
(12) Usta, O. B.; Alexeev, A.; Balazs, A. C. *Langmuir* **2007**, *23*, 10887–10890.
(13) Alexeev, A.; Yeomans, J. M.; Balazs, A. C. *Langmuir* **2008**, *24*, 12102–12106.
(14) Alexeev, A.; Verberg, R.; Balazs, A. C. *Langmuir* **2007**, *23*, 983–987.
(15) Succi, S. *The Lattice Boltzmann Equation for Fluid Dynamics and Beyond*; Oxford University Press: Oxford, 2001.
(16) Ladd, A. J. C.; Kinney, J. H.; Breunig, T. M. *Phys. Rev. E* **1997**, *55*, 3271–3275.
(17) Buxton, G. A.; Care, C. M.; Cleaver, D. J. *Model. Simul. Mater. Sci.* **2001**, *9*, 485–497.
(18) Verlet, L. *Phys. Rev.* **1967**, *159*, 98–103.
(19) Bouzidi, M.; Firdaouss, M.; Lallemand, P. *Phys. Fluids* **2001**, *13*, 3452–3459.
(20) We assign a value of $k/2$ to those springs that are located on the cilia surfaces and $k/4$ to the springs at the edges. We also set the LSM masses to $m/2$ and $m/4$ for nodes at the surfaces and edges, respectively.
(21) Perez-Rigueiro, J.; Viney, C.; Llorca, J.; Elices, M. *Polymer* **2000**, *41*, 8433–8439.
(22) Bureau, L.; Alliche, A.; Pilvin, P.; Pascal, S. *Mater. Sci. Eng., A: Struct. Mater. Prop. Microstruct. Process.* **2001**, *308*, 233–240.
(23) Delaunay, B. N. *Bull. Acad. Sci. USSR: Cl. Sci. Math.* **1934**, *7*, 793–800.

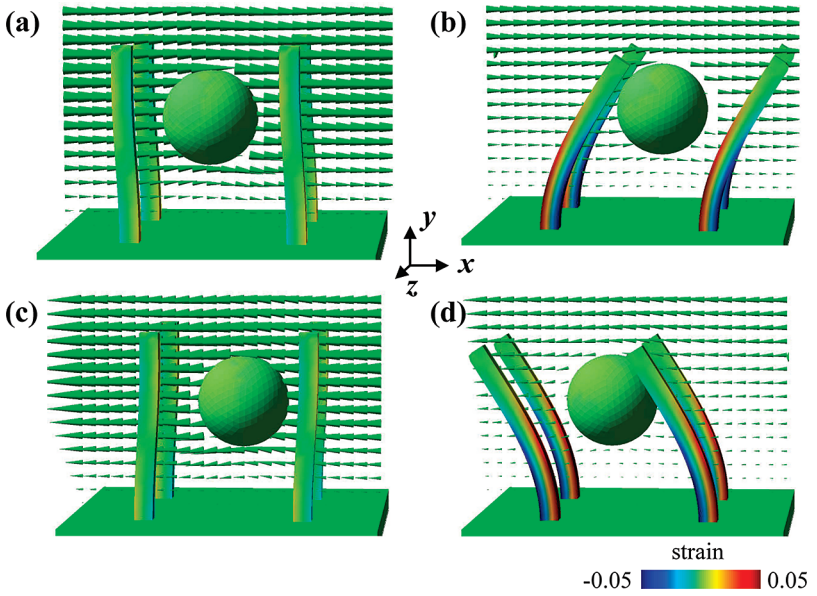

Figure 2. Snapshots from our simulations illustrating periodic oscillations of beating cilia and movement of solid particle for Sp = 3. The colors on the cilium surface show the magnitude of material strain. The arrows indicate the direction and magnitude of fluid velocity at the plane $z = 0$. Panels a, b, c, and d correspond to times $tf = 0$, 0.25, 0.5, and 0.75, respectively.

importance of inertial forces to viscous forces). Descriptions of the dynamic behavior of flexible filaments, such as cilia, are no exception to this practice. In particular, the behavior of cilia is characterized by the dimensionless "sperm number" (see below). Sperm numbers of biological interest[2] and technological relevance[13] typically fall in the 1−10 range. Below, we also adopt the convention of describing the behavior of the cilia via the sperm number; by expressing the data in terms of such dimensionless numbers, we can provide more flexible guidelines for potential experimental studies. In the case of the sperm number, the experimentalist is free to choose, for instance, a combination of cilium size, Young's modulus, and driving frequency that will result in the specified ratio. In the ensuing simulations, we set the simulation parameters so that the values of the sperm number fall in the range noted above.

Results and Discussion

The elastohydrodynamic behavior of beating cilia is normally analyzed in terms of the sperm number, Sp, which characterizes the relative importance of the viscous force and the bending rigidity of oscillating cilia.[24] In particular, $\mathrm{Sp} = L(\zeta\omega/EI)^{0.25}$, where $\zeta = 4\pi\nu\rho$ is the viscous drag coefficient, $\omega = 2\pi f$ is the angular velocity of the driving force, and EI is the bending rigidity of the cilium. In our simulations, we set the fluid density $\rho = 1$ and kinematic viscosity $\nu = 1/6$ (in LB units), and vary f to alter the magnitude of Sp. When Sp is relatively large, the dominant viscous effects suppress the wiggling of the elastic cilia, and, consequently, no net fluid flow is generated. For relatively small Sp, the dynamic shape of the cilium is governed by its elasticity, leading to time-reversible oscillations that are unable to generate net flows at low Re. It is only for intermediate values of Sp, where the effects of cilium elasticity and fluid viscosity are of comparable magnitudes, that a coupling between elastic filaments and viscous fluid permits transport in the low Re environment.

When it comes to synthetic systems, a broad range of polymeric materials can be used to manufacture artificial cilia with sperm numbers in the range of interest. For example, let us consider a cilium that is 20 μm in length and 1 μm in diameter oscillating in water with a frequency of about 10 Hz (which corresponds to biologically relevant frequencies). For such cilia, sperm numbers in the range considered here can be obtained with polymers having a modulus of approximately 2−20 kPa, which is in the range of experimentally realistic values.[8,13,25,26]

Figure 2 shows snapshots from our simulations that illustrate the periodic movement of the compliant, synthetic cilia and solid particle. The height and width of the simulation box are $10R$ and $2(b + B)$, respectively, and we apply periodic boundary conditions along the lateral directions and impose no-slip and no-penetration conditions at the top and bottom walls. At the onset, we place a particle in the center (at $x = 0$, $z = 0$) between four initially quiescent cilia. We then apply the periodic, horizontal force, which drives the cilia to bend back and forth in the $x-y$ plane and thereby induce the movement of the fluid. The viscous fluid, in turn, imposes a periodic drag on the suspended particle. As a result, the particle follows the oscillatory motion of the beating cilia.

Specific trajectories for the particle's center of mass motion are shown for Sp = 3 and Sp = 5 in Figure 3a,b, respectively; as expected, the particles follow oscillatory trajectories. Surprisingly, however, after a short initial transient behavior, the particles steadily migrate in opposite directions across the cilia layer (i.e., along the y-direction). For Sp = 3, the particle moves toward the bottom wall of the microchannel; when we increase the oscillatory frequency to yield Sp = 5, the migration direction is reversed, and the particle moves away from the surface. In other words, by simply changing the oscillating frequency, the actuated cilia can direct solid particles to or away from the channel wall, thereby controlling transport processes inside the ciliated layer.

We characterize the particle migration inside the ciliated layer by measuring U, the period averaged velocity normal to the channel wall. In these simulations, we allow the cilia to oscillate up to 20 periods to avoid the effect of the initial transient behavior. The velocity is shown in Figure 4 as a function of particle distance

(24) Lowe, C. P. *Philos. Trans. R. Soc. London, B* **2003**, *358*, 1543–1550.

(25) Barry, R. A.; Shepherd, R. F.; Hanson, J. N.; Nuzzo, R. G.; Wiltzius, P.; Lewis, J. A. *Adv. Mater.* **2009**, *21*, 2407–2410.

(26) Therriault, D.; White, S. R.; Lewis, J. A. *Nat. Mater.* **2003**, *2*, 265–271.

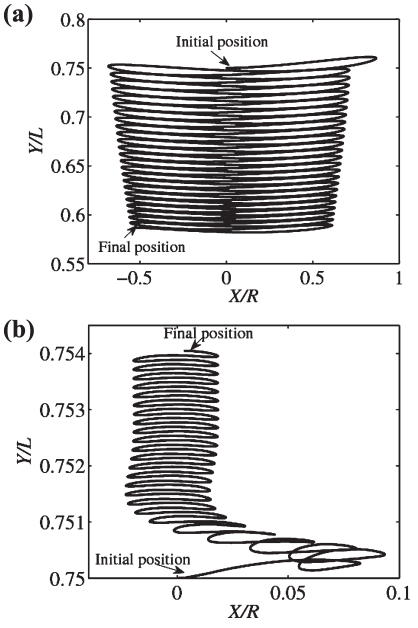

Figure 3. Trajectory of particles during the first 25 periods of cilium oscillations for (a) Sp = 3 and (b) Sp = 5.

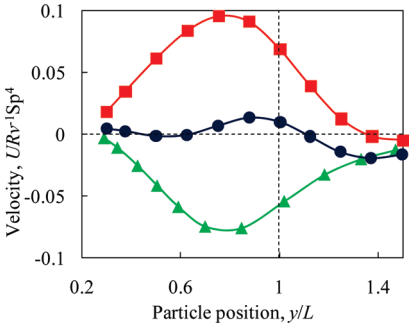

Figure 4. Velocity of particles as a function of distance from the bottom wall. The lines with triangles, circles, and squares show the particle velocities for Sp = 3, Sp = 4, and Sp = 5, respectively.

from the channel wall for different Sp. We normalize the velocities by $Sp^{4-}v/R$ in order to make all the values of comparable magnitude. A positive velocity indicates that the particle is drifting away from the wall. We find that the drift direction indeed depends on the magnitude of Sp. Moreover, for both Sp = 3 and Sp = 5, the velocities do not change sign inside the layer and even slightly above the cilia tips; this behavior indicates that actuated cilia can transport these particles in a unidirectional manner all the way from the channel wall to the outer stream (where the effect of the beating cilia on the fluid flow eventually dissipates).

More specifically when Sp = 3, the actuated cilia can actually trap a particle in the fluid above the layer and bring it into direct contact with the channel surface. In this manner, the cilia can enhance the rate of deposition of suspended particles onto the underlying substrate. Alternatively, cilia oscillating with Sp = 5 can expel particles from the layer and propel them into the outer fluid. In this way, actuated cilia characterized by Sp = 5 can prevent particle accumulation on the surface. We note that when the cilia are oscillating at Sp = 4, the velocity fluctuates around zero, and thus there is little effect of the beating cilia on the net particle displacement relative to the channel wall.

In the above simulations, we placed the particles along a line [$x = 0, z = 0$] in the center of the simulation box and varied the

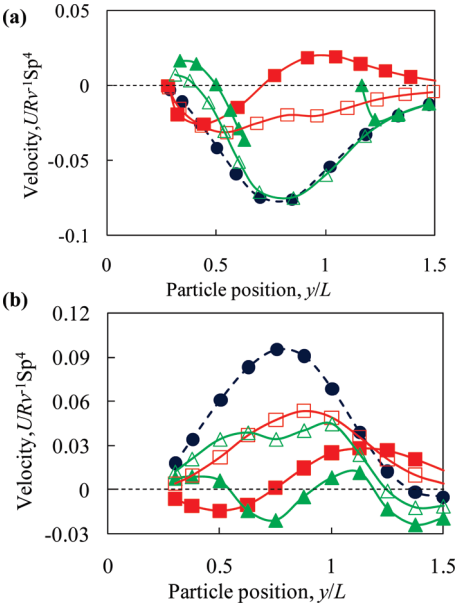

Figure 5. Velocity of particles as a function of distance from the bottom wall for (a) Sp = 3 and (b) Sp = 5. Particles with positive velocity move away from the wall. The dashed lines with filled circles indicate the velocity for particles located at the middle between oscillating cilia $x = 0$ and $z = 0$. The lines with the empty and filled squares indicate particles shifted to $x = 0.5c$ and $x = c$, respectively. The lines with the empty and filled triangles indicate particles at $z = 0.5c$ and $z = c$, respectively.

particle's initial distance from the bottom wall. With the square arrangement of cilia considered here, these particle positions are symmetric relative to the beating filaments and, for this reason, allow particle migration only in the direction normal to the wall. To probe the generality of the observed behavior, it is instructive to investigate the migration of particles that are initially shifted in the x and z directions, i.e., placed along the lines [$x = \delta, z = 0$] and [$x = 0, z = \delta$]. For both Sp = 3 and 5, we plot in Figure 5 the velocities of particles displaced from the center of the domain by distances of $\delta = c$ and $\delta = 0.5c$, where $c = 0.5(B + b)$. Note that $\delta = c$ are symmetry lines, and, therefore, particles located on these lines can only migrate normal to the wall, whereas $\delta = 0.5c$ allows for migration both normal to the bottom surface and in-plane of the layer. For comparison purposes, we also plot in Figure 5 the velocity for particles at [$x = 0, z = 0$].

For Sp = 3 (see Figure 5a), particles along [$x = 0, z = 0$] migrate down to the channel wall. When particles were shifted by $0.5c$ in the z-direction, i.e., normal to the plane of the cilium oscillation, the velocities of the shifted and nonshifted particles are almost identical. When we shifted the particles farther to $z = c$, the oscillating cilia come into contact with particles that are initially located near the cilium height. The latter contacts prevent the particles from moving into the cilial layer. In this case, we cannot measure the velocity since the cilia hit the particles during the first oscillation and push them to a position right above the layer, $y \approx 1.2L$. These situations are indicated by the discontinuity in the velocity profile in Figure 5a. As a result, the particles accumulate above the cilia. On the other hand, those particles that are initially relatively close to the wall, migrate downward and accumulate at $y \approx 0.5L$, where the velocity is zero.

For particles shifted in the x-direction, i.e., parallel to the plane of cilia oscillations, and Sp = 3, we found that for $x = c$, the particles move downward only if they are initially closer than $y = 0.7L$ to the bottom wall. Otherwise, particles are repelled to the outer fluid, although with a velocity that is relatively slow

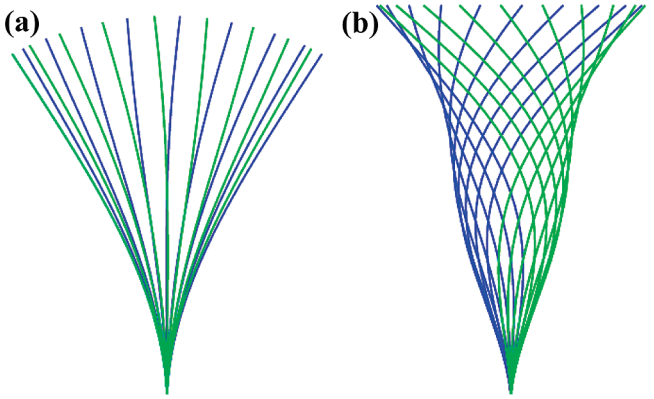

Figure 6. Cilium deformation during one beat cycle for (a) Sp = 3 and (b) Sp = 5. The blue lines show cilia when the force is directed to the right, and the green lines show cilia when the force is directed to the left. For Sp = 5, the horizontal deflection is magnified 10-fold for clarity.

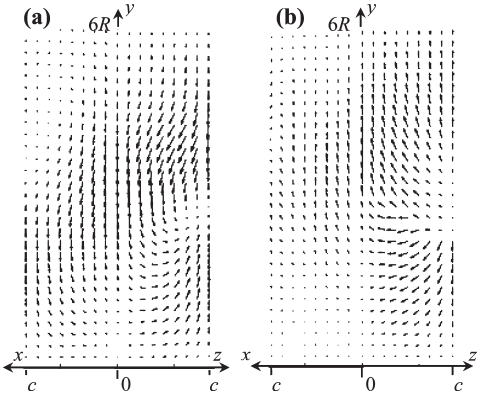

Figure 7. Average velocity field in the middle between the cilia for (a) Sp = 3 and (b) Sp = 5. The velocities have been averaged over one period. The left and right parts of each plot show the $x-y$ and $z-y$ cross sections with the respective velocities.

compared to that at $x = 0$. For particles at $x = 0.5c$, the velocity is always downward, similar to the case for $x = 0$. Interestingly, the velocity at $x = 0.5c$ is approximately the average between the velocities at $x = 0$ and c. (Since the magnitude of the velocity at $x = c$ is smaller than that at $x = 0$, we expect that particles located between $x = 0$ and c will mostly move downward.)

In Figure 5b, we show how the migration velocity changes for Sp = 5 when particles are displaced either in the x or z-direction. For this sperm number, particles in the middle of the domain migrate upward from the solid wall. For $\delta = c$, the velocities are relatively slow and fluctuate around zero. The particles that are initially closer to the cilium tips exhibit positive velocities and migrate out of the layer, whereas particles closer to the channel wall concentrate near this surface. Again, we find that particles at $\delta = 0.5c$ have velocities that are approximately an average of the velocities at $[x = 0, z = 0]$ and $\delta = c$, and always move away from the bottom wall. Hence, for Sp = 5, the actuated cilia will propel the particles away from the wall, except for a few cases where the particles are located between pairs of beating cilia (see Figure 5b).

To gain insight into the effects that contribute to the controllable migration of the particles with changes in Sp, we examined the oscillatory patterns for an individual cilium at both Sp = 3 and 5. Figure 6 reveals that indeed the cilium exhibit different dynamical behavior at these different Sp values. In particular, at Sp = 3, the cilium makes extensive excursions in both the forward and backward motion. At the higher Sp, however, the effect of viscous damping is more pronounced, and the cilium makes smaller deviations in the lateral direction. Furthermore, Figure 6 shows that the change in Sp alters the mode of cilium bending. It is noteworthy that the oscillations for Sp = 3 and 5 correspond to the first two oscillatory modes of a beating flagellum,[27] and this motion generates traveling waves that transport the fluid along the cilium.[27,28]

Various studies indicate that changes in Sp affect not only the oscillatory behavior of the tethered filaments, but also the fluid flow within the system.[13,27,29−31] Namely, theoretical calculations show that a magnetically actuated swimmer, which contains a spherical head and elastic flagellum, alters its direction of motion with changes in the driving frequency f (and hence Sp).[29] Furthermore, we previously examined the dynamic behavior of cilia that were tilted with respect to the substrate and actuated by a periodic vertical force applied to the cilium free ends[13] and found that, by changing Sp, we could switch the direction of the net flow within the microchannel. Similar results were predicted for magnetically actuated artificial cilia.[30]

Consequently, we correlate the reversal of the particle's motion to changes in the cilium mode of oscillation that lead to changes in the flow patterns. Since the cilia considered herein are tethered normal to the solid surface, no *net* flow is generated within the system. Our simulations indicate, however, that the undulating filaments induce circulatory secondary flows in the liquid and that the direction of these flows is controlled by the mode of filament motion. To explore this effect, we introduced size-less tracer particles into the fluid and measured the flow velocities inside the cilial layer.

As seen in Figure 7, where we plot the period averaged tracer velocities, the direction of flow circulation indeed depends on the magnitude of the sperm number. Specifically for velocities in the midplane between the actuated cilia, the flow is directed downward when Sp = 3 and upward for Sp = 5. These flow patterns agree with the directions of motion for the solid particles shown in Figures 4 and 5.

Without particles, the flow patterns that emerge among oscillating filaments are determined by the magnitude of the sperm number and the grafting density of cilia on the substrate. When solid particles are introduced, however, they modify the local flows, and the relative size of these particles becomes an important parameter controlling the particle migration and deposition. The fluid continuity and the impenetrable boundary condition imply that the averaged fluid flow close to a cilium surface and in the gap between cilia have opposite directions. For the relatively large particles considered here, the spheres remain in the middle between oscillating cilia due to geometrical constraints and thus follow the fluid flow arising in this location. This behavior, in turn, results in the observed unidirectional migration of the large particles in the ciliated layer. In contrast, solid particles that are much smaller than the cilium size would have less effect on the surrounding fluid and thus, could follow circulatory streamlines within the layer. In this situation, only those particles that come closer than one particle radius to the solid walls could potentially deposit on these surfaces; otherwise, the smaller particles will continuously circulate with the fluid inside the cilial layer.

(27) Wiggins, C. H.; Riveline, D.; Ott, A.; Goldstein, R. E. *Biophys. J.* **1998**, *74*, 1043–1060.
(28) Lauga, E.; Powers, T. R. DOI: arXiv:0812.2887v1 [cond-mat.soft] **2008**.
(29) Alexander-Katz, A. DOI: arXiv:0705.2669v1 [cond-mat.soft] **2007**.
(30) Gauger, E. M.; Downton, M. T.; Stark, H. *Eur. Phys. J. E* **2009**, *28*, 231–242.
(31) Fu, H. C.; Powers, T. R.; Wolgemuth, C. W. *Phys. Rev. Lett.* **2007**, *99*, 258101.

We, therefore, expect that the effect of actuated cilia on particle migration might decay with decreasing particle size. We will consider this behavior in more detail in future studies.

Conclusions

In summary, we find that actuated cilia can control the transport of solid particles near the substrates of microfluidic channels. For low frequency oscillations characterized by a sperm number of Sp = 3, the cilia effectively draw particles from outside the layer and deliver these species to the underlying surface. For larger frequencies characterized by Sp = 5, the cilia expel the particles and therefore can be used to clean the ciliated surface from foreign entities and inclusions.

We show that the migration of neutrally buoyant particles is due to secondary flows excited by periodically oscillating filaments and that the direction of these flows controls the direction of particle transport. We find that the flow direction changes between Sp = 3 and 5 and associate this change with different modes of cilium oscillations. We note that these hydrodynamic effects are limited in range and primarily affect particles that are relatively close to the ciliated surface.

It is noteworthy that on a very general level, our results show qualitative agreement with observations that the capture of food particles by certain suspension feeders is most effective for a finite range of ciliary beat frequencies.[3] Furthermore, it is worth noting that behavior similar to what we find for Sp = 5 has been observed experimentally in a microfluidic device that utilizes actuated synthetic cilia.[6] In particular, the researchers detected an upward migration of suspended microscopic particles when the cilia are driven to beat at frequency of 65 Hz. The arrangement and size of the cilia in these experiments, however, are sufficiently different from the scenario considered here that it is difficult to make a direct comparison between our simulation results and the experimental findings. Moreover, the latter experimental study did not report any changes in the particle migration with variations in the frequency of oscillation. We hope that the findings presented here can motivate further experimental studies to probe the effect of actuated filaments on particle motion in microchannels.

In addition to revealing new methods for manipulating particles for lab-on-a-chip applications, our studies can also provide some insight into factors that control the interactions between cilia in the respiratory tract and particulates such as dust or mucous. In particular, it has been reported that certain chemicals can increase the ciliary beat frequency and consequently, the cilia-driven particle transport within the trachea of mice.[32] The physical mechanism for this behavior is not completely understood; ultimately, computational studies such as those described herein could reveal fundamental principles that contribute to the effective removal of unwanted particulates from the respiratory system.

Acknowledgment. A.C.B. gratefully acknowledges financial support from the ONR.

(32) Konig, P.; Krain, B.; Krasteva, G.; Kummer, W. *PLoS One* **2009**, *4*, e4938.